

Photoelectron-spectroscopy study of the electronic structure of Au and Ag overlayers on Pt(100), Pt(111), and Pt(997) surfaces

M. Salmerón,* S. Ferrer,* M. Jazzar,[†] and G. A. Somorjai

*Materials and Molecular Research Division, Lawrence Berkeley Laboratory, Berkeley, California 94720
and Chemistry Department, University of California, Berkeley, California 94720*

(Received 1 July 1983)

We have used photoelectron spectroscopy techniques [UPS (ultraviolet) and XPS (x ray)] to study the electronic structure of Au and Ag overlayers deposited on Pt(100), Pt(111), and Pt(997). Between 0 and 1 monolayer, the valence bands of Au and Ag show changes in the form of shifts of the most tightly bound peaks and the appearance of new structures around a coverage $\Theta=1$ monolayer. The Au $5d_{3/2}$ peak shifts 0.6 eV towards higher binding energies when Θ varies from 0.1 to 1 monolayer and 0.5 eV more when Θ varies from 1 to 6 monolayers. In the case of Au on Pt(100) a shallow minimum in the work function around $\Theta=1$ monolayer is observed. The $4f$ core levels of Au on Pt(100) shift also to higher binding energy as Θ increases. From $\Theta=0$ to 1 monolayer the shift is 0.6 eV and from $\Theta=1$ to 4 monolayers additional 0.4-eV shift is observed. These shifts are explained as due to the changing contributions of the Au atoms in island edges for surface ($\Theta < 1$) and bulk ($\Theta > 1$) coordination positions.

I. INTRODUCTION

The production of well-controlled atomic thin layers of metals deposited on a single-crystal substrate offers unique possibilities to study the electronic and chemical properties of small metal clusters using surface-science techniques such as Auger, low-energy electron-diffraction (LEED), and photoelectron spectroscopies. The electronic structure of these clusters will be affected both by the reduced average coordination number^{1,21,22} and by the interaction with the support. For example, it has been established on the basis of photoemission experiments, that the electron binding energies of surface atoms in a solid material can be different from the ones corresponding to atoms located in the bulk.¹⁻³ Surface-bulk binding-energy shifts have already been observed for core and valence-band levels of gold.^{1,4} We will show here how the deposition of monolayer and submonolayer amounts of gold and silver on various Pt crystal surfaces can be used to observe the influence of the reduced coordination of the gold atoms in going from bulk to surface and step-edge atomic positions. These observations can be used in determining the degree of dispersion of gold in the submonolayer regime.

The case of Au overlayers is particularly interesting also, in view of the surface reconstructions observed in both substrate and adsorbate that depend on the coverage of Au. Sachtler *et al.* have shown⁶ that the LEED pattern of the reconstructed Pt(100), i.e., the "1×5" structure changes upon Au deposition to 1×1 at a coverage of $\Theta=0.5$ and remains so up to $\Theta=2$. (The coverage will henceforth be given in units of monolayers.) Above this coverage a 1×7 pattern due to the gold layer is observed; it remains unmodified up to coverages as high as 30 monolayers.⁶

The chemical properties of both substrate and overlayers can be also strongly modified in connection with

the atomic thickness of the overlayer as compared to the surfaces of the corresponding bulk materials. This has been seen in some instances as in the systems Pd/Nb(110) (Ref. 7) and Pd/W(110),⁸ and also the Ag/Pt(100), Ag/Pt(111), Ag/Pt(553), Au/Pt(100), Au/Pt(111), and Au/Pt(553) surfaces towards the chemisorption of simple molecules such as CO, O₂, and H₂.⁹ The reactivity of the Au/Pt(100) system for the dehydrogenation of cyclohexene to benzene was also studied in this laboratory as a function of Au coverage.¹⁰ It was found that the reactivity increases upon Au deposition and reaches a maximum at the monolayer coverage to decrease thereafter to zero as the Au coverage increases beyond two monolayers.

II. EXPERIMENTAL SETUP

The experiments were performed in a UHV chamber with a base pressure of 1×10^{-10} Torr. It was equipped with LEED, x-ray photoelectron spectroscopy (XPS) with double-pass cylindrical-mirror-analyzer (CMA) and Auger-electron spectroscopy. The same electron energy analyzer was used also for ultraviolet photoelectron spectroscopy (UPS). A He resonance lamp provided a grazing beam of photons of 21.2 eV. The chamber was also equipped with a UTI quadrupole mass spectrometer for residual gas analysis. The Pt single crystals were spark-cut from a single-crystal bar and oriented within $\pm 1^\circ$ of the desired orientation by means of x-ray Laue diffraction. The samples were of approximately 1 cm² in area and 0.5 mm thick. Inside the vacuum chamber three Pt single crystals of (100), (111), and (997) orientations were mounted in a carousel-type manipulator. Cleaning of the crystals was achieved by a combination of argon-ion sputtering and heating in O₂ partial pressures in the 10⁻⁷-Torr range. After these treatments the crystal was heated to high temperature of the order of 1300 K to remove oxygen and to anneal the surface.

Deposition of gold and silver was performed by resistively heating a tungsten wire wrapped around the noble metals that were previously melted inside the wire.

The growth of the deposits was followed by Auger spectroscopy and we found thus that Au grows layer by layer. This result agrees very well with the previous one by Sachtler *et al.*⁶ in this laboratory.

Similarly, Ag deposition was controlled by Auger spectroscopy and use was made of the calibration performed in this laboratory for the same system by Davies *et al.*⁹

III. RESULTS

A. Photoelectron spectra of Au layers on Pt(100)

In Fig. 1 we show the clean Pt(100) electron distribution curve ($\Theta=0$) in integral form for photons of 21.2-eV energy which are incident at grazing angles to the Pt crystal surface. The spectrum is largely integrated due to the fairly large acceptance angle of the CMA. The spectrum of clean Pt(100) (reconstructed 1×5) is characterized by a sharp increase near the Fermi level followed by a series of peaks arising from *d*-band-derived transitions. The work function was measured to be 5.82 ± 0.15 eV. In the same figure we show the difference spectra (Au/Pt minus clean Pt) corresponding to various Au coverages, as indicated in

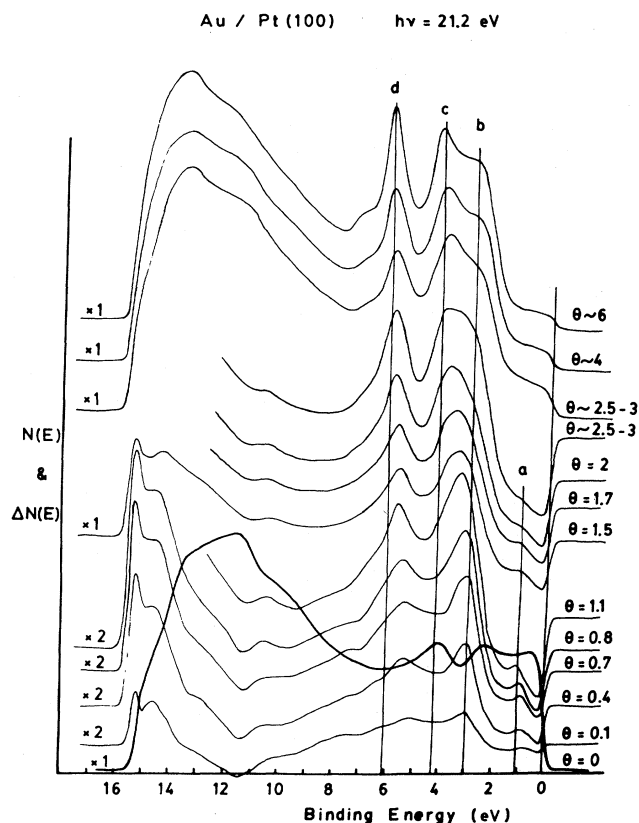


FIG. 1. Photoemission spectra of Au overlayers on Pt(100) using HeI radiation. Gold coverage Θ is indicated at the right-hand side of each curve. Thick solid curve for $\Theta=0$ corresponds to the clean substrate and is shown in integral form. Curves for $\Theta=0.1-2$ are shown in difference form only.

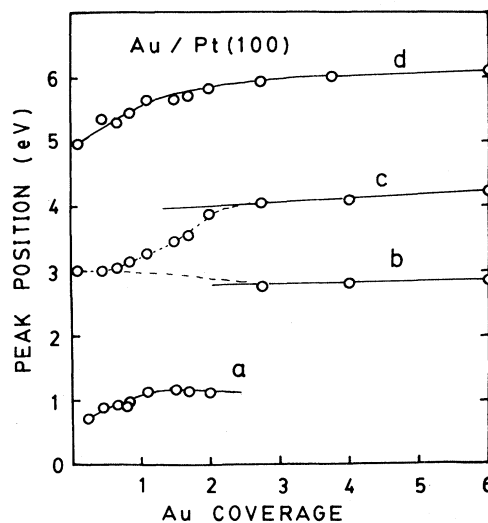


FIG. 2. Binding energy of the various peaks due to Au in Fig. 1 as a function of coverage for the Pt(100) substrate. Curves similar to these were obtained for the two other substrate orientations.

the right-hand side of the figure. In order to compensate for the attenuation of the Pt signal due to the Au overlayer, the intensity of the clean Pt spectrum was scaled down by using an attenuation factor derived from the universal mean-free-path curve of electrons of energy between 10 and 15 eV. This procedure, however, produced only minor changes in the difference curves as compared to a direct subtraction, i.e., without correction for attenuation. Only at coverages above $\Theta=2$ the effects of the scaling were clearly noticeable. At this point, however, we present the spectra in its integral form as shown in the figure.

At coverages between 0 and 1 the spectra due to the Au overlayers are characterized by three main peaks at energies of approximately 1 eV (peak *a*), 3 eV, and 5 eV (peak *d*) at the lowest coverage. The energies of these peaks change as a function of coverage as shown in Fig. 2. Peak *a* shows an interesting behavior: Apart from shifting from 0.7 to 1.2 eV its intensity increases up to a maximum value at $\Theta=1$, then it decreases to zero at coverages between 2 and 3. The other two peaks shift also to higher binding energies, as shown in Figs. 1 and 2. The shift of peak *d* amounts to 0.6 eV between $\Theta=0.1$ and 1 and an additional 0.5 eV from $\Theta=1$ to $\Theta \approx 6$. The behavior of the peak initially at 3 eV is complicated by its overlap with a new peak that grows up at coverages around $\Theta=1$. With further gold deposition these two peaks separate and give rise to peaks *b* and *c* shown in Fig. 1.

The work function Φ , which is measured from the position of the onset of the secondary electron cascade, also shows an interesting behavior as a function of Au coverage. The result is shown in Fig. 3. After a rapid decrease for small Au coverages it goes through a minimum, 0.48 eV below the clean surface value, at coverages near unity. It recovers its thick-layer value at coverages between 2 and 3. It should be noticed that the absolute error bar shown

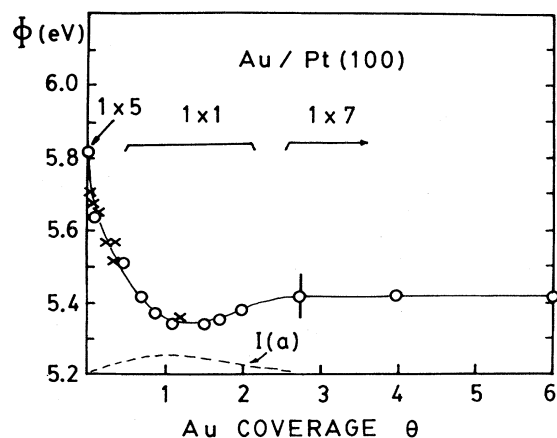


FIG. 3. Work function of Pt(100) covered with Au as a function of coverage as measured from the onset of the electron cascade in the curves of Fig. 1. Intensity of peak *a* of Fig. 1 is also shown as broken line. On top are indicated the LEED structures formed.

in the figure is larger than the depth of the minimum (0.07 eV), whereas the relative error is of the order of 0.05 eV. The behavior of the intensity of peak *a*, at 1 eV below the Fermi level, is also shown in Fig. 3. The LEED patterns observed by Sachtler *et al.*⁶ in the same coverage ranges are also indicated in the figure.

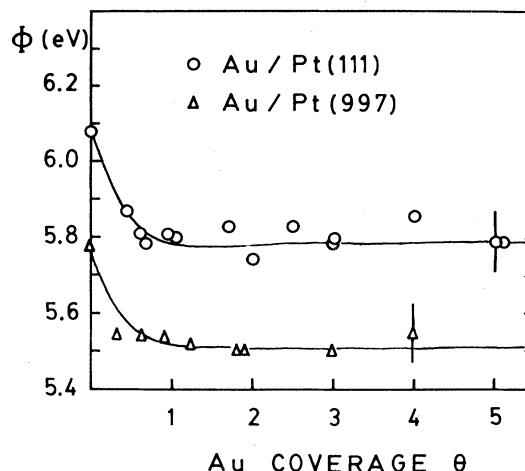


FIG. 5. Work-function variation of Pt(111) and Pt(997) as a function of Au coverage.

Finally, the intensity of the emission at the Fermi edge was also measured as a function of Au coverage. It was found that it decreased monotonically with Au coverage from $\Theta=0$ to 6. This observation has some implications as to the structure of the Pt and Au surfaces as will be shown in the discussion section.

B. Photoelectron spectra of Au layers on Pt(111)

The spectra corresponding to clean and Au-covered Pt(111) are shown in Fig. 4. The clean surface is characterized by a sharp increase of emission upon crossing the Fermi-level line. It differs from that of Pt(100) by a sharp peak 0.4 eV below the Fermi level. The work function was measured to be 6.08 ± 0.15 eV.

The photoemission spectra due to Au overlayers are shown in the same figure in difference form. At low Au coverages the spectra consists of peaks at binding energies of 5.5 eV (peak *d*), 3 eV, and two smaller peaks at 1.9 and 0.8 eV (*a* and *a'*). The behavior of these peaks as the gold coverage increases is the following: The peak at 5.5 eV shifts to higher binding energies to reach a final multilayer value of 6 eV; the peak at 3 eV is accompanied at Au coverages between 0.6 and 1 by new structures that grow in intensity until the final form consisting of the two peaks marked *c* and *b* is obtained at multilayer coverage.

The two small peaks *a* and *a'* are visible only up to approximately one Au monolayer. At Au coverages around two monolayers they are already negligible. The work function decreased upon gold deposition from its initial value of 6.08 eV down to 5.8 eV. That value was reached at the monolayer and remained constant thereafter, as shown in Fig. 5.

C. Au/Pt(997)

A very similar behavior was observed in the case of the stepped Pt(997) surface. In Fig. 6, we show the photoemission curves corresponding to clean and gold-covered Pt(997). The clean-surface spectrum is characterized by an intense peak at 0.4 eV below E_F . The intensity of this

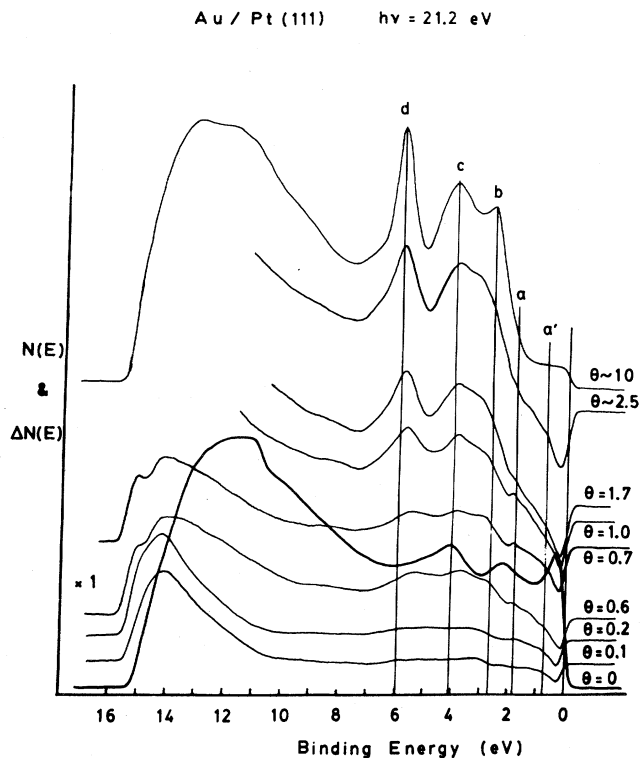


FIG. 4. Photoemission spectra of Au overlayers on Pt(111). Coverage Θ is indicated on the right-hand side. Thick line curve for $\Theta=0$ and the top curve for $\Theta \sim 10$ are shown in integral form. For intermediate coverages only the difference spectra are shown.

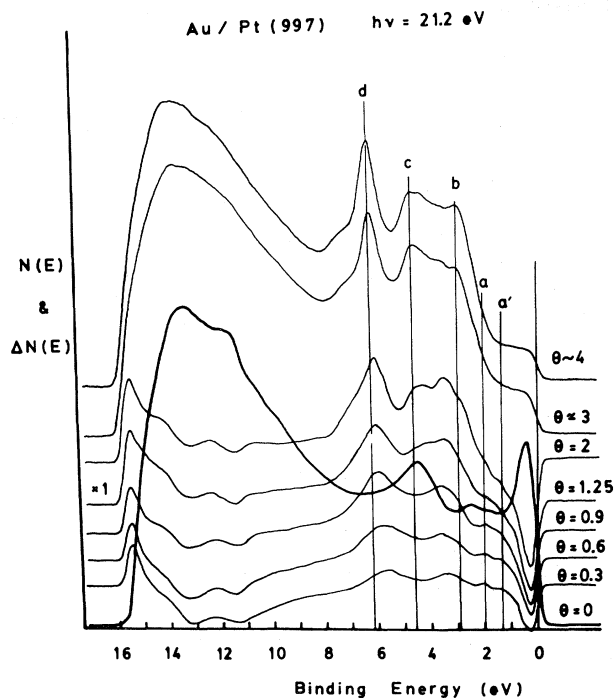


FIG. 6. Photoemission spectra of Au overlayers on Pt(997) for various coverages Θ as indicated on the right-hand side. Difference curves are shown except for $\Theta=0$ (thick solid line) and $\Theta > 3$. Notice the intense emission peak near the Fermi level in the clean-surface spectrum.

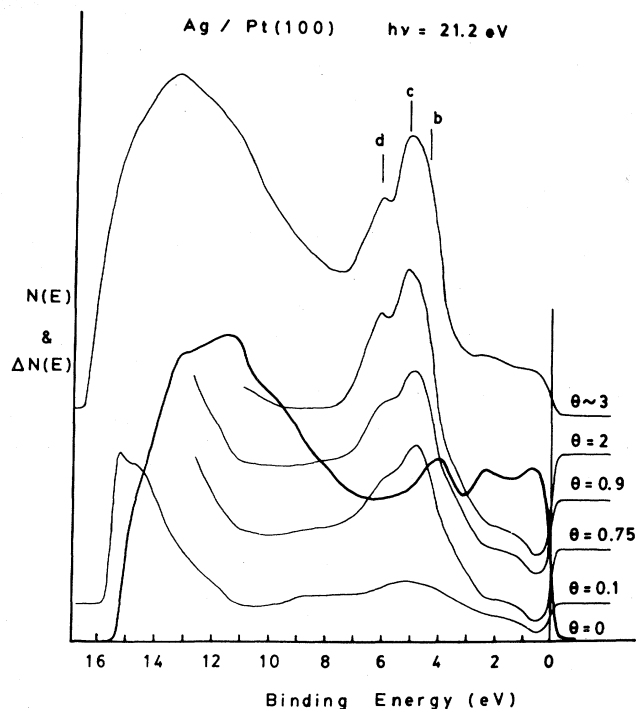


FIG. 7. Photoemission spectra of Ag overlayers on Pt(100) as a function of coverage Θ as indicated on the right-hand side. Thick solid line corresponding to $\Theta=0$ and the top curve for $\Theta \sim 3$ are shown in integral form. For intermediate coverages only difference curves are shown.

peak is noticeably higher than that of the similar peak observed in Pt(111) (Fig. 4). The work function for this stepped surface was measured to be 5.78 ± 0.15 eV. Upon gold deposition this value decreased in a way similar to the (111) surface as shown in Fig. 6. It reached a final value of 5.5 eV when the gold coverage was approximately 1.

The difference spectra corresponding to various gold coverages is characterized, at the lowest coverages, by peaks at binding energies of 5.5, 3.3, 1.9, and 1.4 eV. The peak at 5.5 eV shifted to higher binding energies for increasing gold coverages to reach a final position of 6.2 eV (peak *d*). Most of the shift occurred in the range of 0–2 monolayers. The peak initially at 3.3 eV is accompanied by new peaks that grow when the Au coverage approaches the monolayer, as can be seen in Fig. 6. At higher coverages these peaks grow to produce the final multilayer structure in the region marked by peaks *c* and *b*. As in the case of the (111) substrate the small features between 1 and 2 eV below E_F (*a* and *a'*) are visible at the lowest coverages and disappear for Au coverages between 1 and 2.

D. Ag layers on Pt(100) and Pt(997)

The photoemission spectra of clean and Ag-covered Pt(100) and Pt(997) are shown in Figs. 7 and 8. The difference curves reveal that at very low coverages ($\Theta \approx 0.1$) the spectrum consists mainly of a broad peak

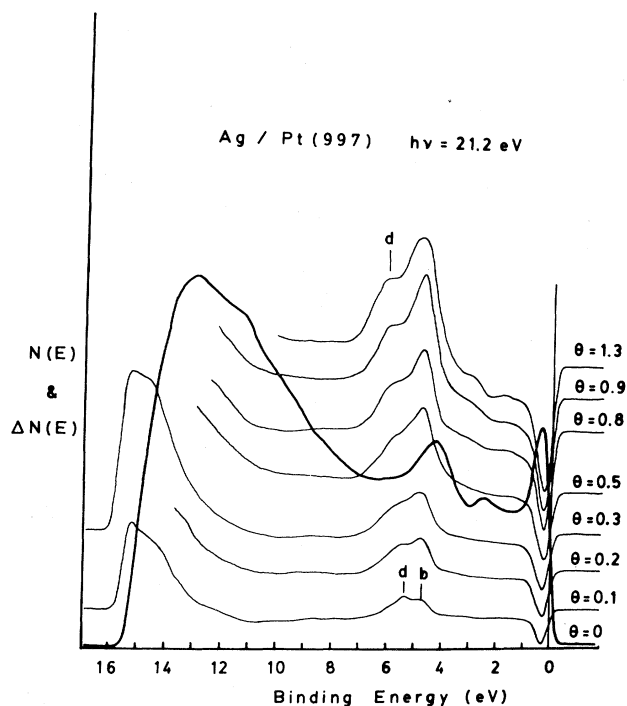


FIG. 8. Photoemission spectra of Ag overlayers on Pt(997) in difference form. Coverages Θ are indicated on the right-hand side. Thick solid line corresponding to the clean stepped substrate is shown in integral form.

centered at approximately 4.9 eV below E_F for both substrate orientations. In the case of Pt(997) this peak can be seen as composed by two neighboring peaks with maxima at 4.70 (peak *b*) and 5.4 (peak *d*). As the Ag coverage increases the two peaks evolve in a fashion which is similar to the behavior of the Au/Pt system. Thus, whereas the peak at 4.70 eV varies in position only slightly, the peak at 5.46 eV shifts rapidly to higher binding energies (close to 6.1 eV above $\Theta=1$). Most of the shift occurs in the first monolayer. Above $\Theta=1$ also, the peak at 4.7 eV becomes wider and assymmetric as a result of its decomposing into two peaks centered at approximately 5.15 (peak *c*) and 4.70 eV (peak *b*). This behavior is similar to that found for peaks *b* and *c* of Au on Pt. The results for Ag are shown in Fig. 9(a). The work function of clean Pt(100) was found to decrease rapidly from 5.82 to 4.76 eV at $\Theta=1.0$ as shown in Fig. 9(b). After that it rapidly reaches its multilayer value of 4.71 eV.

No minimum in Φ is observed. The intensity of the photoemission curve at E_F decreased monotonically with coverage. In the case of the Pt(997) substrate the behavior was very similar. The work function decreased continuously from its clean-surface value of 5.78 to 4.82 eV at $\Theta=1.3$ [see Fig. 9(b)]. No further deposition of Ag was performed in that case. Here also the intensity at the Fermi level decreased monotonically with Ag coverage.

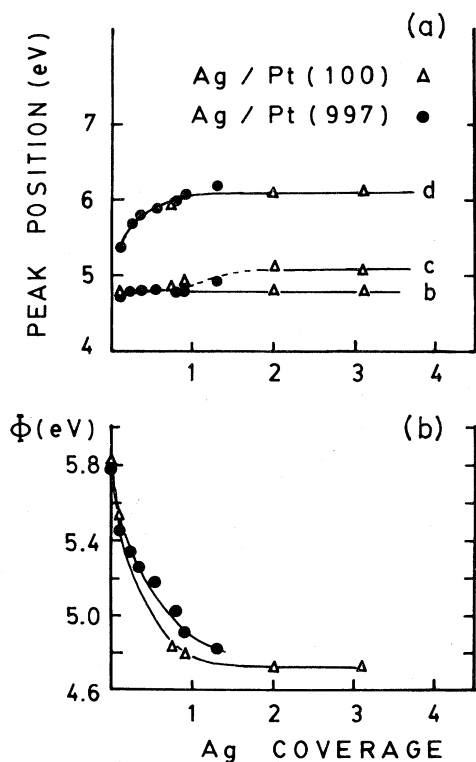


FIG. 9. (a) Binding energy of the various peaks due to Ag in the photoemission curves of Figs. 7 and 8 as a function of coverage. Only the peak labeled *d* shows a noticeable shift in the range $0 < \Theta < 1$. (b) Work-function variation of Pt(100) and Pt(997) as a function of Ag coverage.

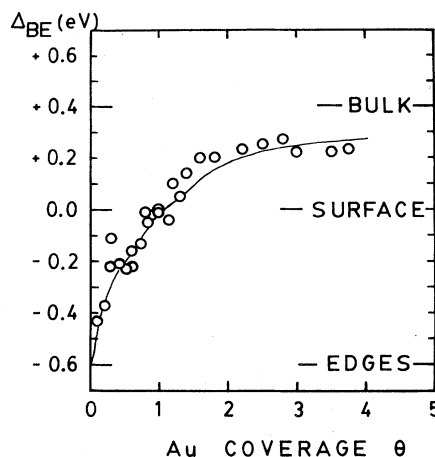


FIG. 10. Binding-energy shifts, Δ_{BE} , of the 4*f* core levels of Au relative to the monolayer of gold as a function of coverage. Continuous curve is the result of a calculation where the photoelectron peak is assumed to be composed of three peaks due to Au atoms in island edge (for $\Theta < 1$) surface and bulk coordination (for $\Theta > 1$) positions.

E. XPS results for Au/Pt(100)

The Au/Pt(100) system was also studied with XPS. Both the 4*f*_{7/5} and 4*f*_{5/2} photoelectron lines of Pt and Au were monitored as a function of gold coverage.

In order to eliminate errors in the absolute values of the binding energies the position of the Au 4*f* lines were measured relative to the nearby lines of the Pt substrate. A continuous shift towards higher binding energies was found as the Au coverage increased from 0.1 to 4 monolayers, as shown in Fig. 10. The total shift observed is 0.70 ± 0.15 eV, with 0.43 eV occurring from $\Theta=0.1$ to 1 and the remaining 0.25 eV from 1 to 4 monolayers.

It is important to note here that the Mg *K* α x-ray line used in these experiments is rather wide in energy. Our 4*f* photoelectron peaks for Au and Pt have a full width at half maximum (FWHM) of 1.25 eV. This, of course, prevents the observation of individual peaks with energy separation of less than approximately 1 eV.

IV. DISCUSSION

A. Photoemission results from Au overlayers

The first observation common to all three Pt substrate orientations is the appearance, at coverages below one Au monolayer ($\Theta=1$), of three main features that evolve in a different way with increasing Au coverage. These are the peaks around 5–6 eV, 3–4 eV, and below 2 eV. The highest-binding-energy peak, initially at 5 eV, is part of the Au 5*d*_{3/2}-derived subband and shows a continuous shift of 1.1 ± 0.1 eV in going from $\Theta=0.1$ to $\Theta \approx 6$. Since this peak is at the highest-binding-energy end of the observed spectra, its shift implies a continuous narrowing of the density of states when the average coordination number of the Au atoms decreases. The shift of 0.5 ± 0.1 eV observed for all three Pt substrates between $\Theta=1$ and 6 is in excellent agreement with the findings of Citrin *et al.*¹

who were able to obtain the first-layer contribution to the photoemission curves of Au (in an evaporated film). By subtracting two conveniently weighted curves corresponding to normal and grazing emergences they could measure a narrowing in the density of states when going from bulk to one atomic layer of Au of 0.5 eV. The polycrystalline nature of their film does not invalidate the comparison as the 0.5-eV shift was measured (from $\Theta=1$ to multilayers) for the three substrate orientations. In fact, their deduced curve for the first gold layer compares very well with our $\Theta=1.1$ curve in Fig. 1, as already shown in our previous paper.¹¹ It is very interesting to observe that the prediction of band narrowing with decreasing size of the gold cluster, i.e., below one monolayer, is indeed fulfilled. This is the first instance to our knowledge where the effect of the decreasing size of two-dimensional gold islands (for $\Theta < 1$) is observed to produce an additional narrowing of the density of states. The second feature of interest in the photoemission curves due to Au is the region around 3–4 eV in the three Pt substrates (Figs. 1, 4, and 6). This region contains only one peak for the lowest Au coverages in the three cases. For the Pt(100) substrate, this peak shows only a small shift between $\Theta=0.1$ and 1 (see Fig. 2). Near this last coverage and above, however, there is a clear shift to higher binding energies which is due to the growth of new peaks in this region of the spectrum. At coverages above 2, the shape of the spectrum is already very similar to the multilayer one that contains two main peaks marked *c* and *b* in Figs. 1, 4, and 6. Whereas in the Pt(100) and Pt(997) substrates the appearance of the new peaks occurs very close to $\Theta=1$, in the (111) substrate they are already visible at $\Theta=0.6$. This may be due to either imperfect layer-by-layer growth or to unaccounted errors in the Au-coverage measurement. Clearly, the appearance of new peaks in this region upon crossing the monolayer coverage must reflect the formation of Au–Au bonds between layers, whereas the original peak at around 3 eV must be originating from the bands formed by the Au–Au bonds within the layer.

The region of the photoemission curves due to Au between the Fermi level and 2 eV is also interesting. In the Pt(100) substrate, one peak (marked *a* in Fig. 1) is observed that grows with increasing Au coverage up to $\Theta=1$. Since this peak lies well above the *d*-band region it could be due to a surface state derived from *sp*-type orbitals. Peaks due to surface states were observed for both normal and reconstructed Au(100) by Heimann *et al.* at around 1.7 eV (Ref 12) using angle-resolved photoemission. However, as is visible in Fig. 1, peak *a* is located in a region of negative values of the difference spectrum, and therefore it does not actually correspond to a gold-induced emission but rather to a selective depletion of substrate electrons by deposited Au. As a consequence the identification of peak *a* as a surface state seems unappropriate. This remark is not valid for the two other substrate orientations which also show small peaks in that region of the spectrum (*a* and *a'* in Figs. 4 and 6) whose intensities follow a similar trend to that of peak *a* in the Pt(100) substrate. In the other cases, however, both *a* and *a'* peaks correspond to weak *positive* emissions.

B. Substrate Pt(100) reconstruction

There is another interesting conclusion that can be drawn from the observations regarding the observed LEED structures and the density of states at the Fermi level. The sequence of surface structures observed by Sachtler *et al.*⁶ is indicated in Fig. 3 as a function of gold coverage. One question that arises from this observation is whether or not the observed 1×1 patterns correspond to the formation of 1×1 unreconstructed domains of Pt(100) in the surface patches not covered with Au, in addition to the Pt areas beneath the Au islands. This question is related obviously to the local versus long-range character of the reconstruction of metal surfaces. Bonzel *et al.*¹³ showed that the unreconstructed 1×1 Pt(100) surface gives rise to an intense photoemission peak very close to the Fermi edge that is not present on the reconstructed 1×5 surface. The intensity of this peak is high enough to be unambiguously observable in our spectra, in the range $0 < \Theta < 1$, should the uncovered Pt areas have the 1×1 structure. The fact that the intensity of emission at the Fermi edge was observed to decrease monotonically as Θ increased, proves that the uncovered Pt areas retain the 1×5 reconstruction. The disappearance of the fractional spots in the LEED pattern in the range $0.5 < \Theta < 1$ can be explained by the reduced number of unit cells that can be accommodated in the uncovered patches of the Pt substrate. This is particularly so because of the large dimensions of the " 1×5 " unit cell.

C. Work-function results

Inspection of the variation of the work function Φ with Au coverage (Figs. 3 and 5) shows that its decrease is larger than the linear interpolation between the values at $\Theta=0$ and 1. This observation, together with the layer-by-layer growth of Au, indicates that the observed deviation from linearity must be due to the large number of step edges of Au islands present in the submonolayer range. Besocke *et al.*¹⁴ and also Gardiner *et al.*¹⁵ have shown that for Au, Pt, and W stepped surfaces, the contribution of the dipole moment associated with the steps to the decrease in Φ is linear with increasing step density on a fairly large range. This result will be used below to obtain an estimate of the total island perimeter.

In the case of the Pt(100) substrate, the clean surface value of Φ , 5.82 ± 0.15 eV, compares very well with the value of 5.84 eV reported by Nieuwenhuys *et al.*¹⁶ The final multilayer value (above $\Theta=2$) of $\Phi=5.42 \pm 0.15$ eV is similar to that reported by Potter *et al.*¹⁷ for Au(100), namely 5.47 eV. Interestingly though, a shallow minimum 0.07 eV below the multilayer value is observed around $\Theta=1$. One possible explanation is that this lower value of Φ reflects the more open nature of the 1×1 structure that is observed with LEED in this coverage range. Above $\Theta=2$, a reconstructed 1×7 structure is observed that is interpreted as a quasihexagonal overlayer of Au on the square substrate, similar to the familiar " 1×5 " structure.⁶

The initial, clean substrate value of Φ for the Pt(111) surface, 6.08 ± 0.15 eV, compares only fairly with that reported by Ertl¹⁸ of 6.40 eV. Its smaller value might re-

flect a less perfect surface with a larger number of residual steps. Other values found in the literature, such as that of Nieuwenhuys *et al.*¹⁶ of 5.93 eV, are smaller than our measured value. The multilayer value found for that substrate orientation of 5.80 ± 0.15 eV is clearly larger than the 5.31-eV value reported by Potter *et al.*¹⁷ for bulk Au(111).

The stepped platinum (997) surface gave a value of $\Phi = 5.78 \pm 0.15$ eV for the clean surface. This value is smaller than that found for the flat (111) surface and is consistent with the general trend towards lower work functions that is found in the surfaces with steps and irregularities.¹⁴ In fact, the decrease in Φ from the (111) to the (997) surface, with a step density of 5×10^6 cm⁻¹, is ~ 0.30 eV, a value very similar to the decrease in Φ measured by Besocke *et al.*¹⁴ The multilayer Au deposit ($\Theta \sim 4$) on this stepped surface gave a value of $\Phi = 5.52 \pm 0.15$ eV which is smaller by 0.27 eV than that corresponding to the flat substrate. Although no LEED check was performed as to the possibility of steps in this Au multilayer, the decrease in Φ with respect to the (111) multilayer can be compared to that measured by Besocke¹⁴ of $\Delta\Phi = 0.17$ for the Au(111) stepped surface of the same step density relative to the flat (111) surface.

As mentioned above, the deviation from linearity in the decrease of Φ between $\Theta = 0$ and 1 can be used to estimate the total perimeter of the gold islands. To do that several simplifying assumptions were made. Firstly, it was assumed that, as in the case of the stepped Pt, Au, and W surfaces, the deviation is proportional to the step density, i.e., to the total perimeter length in our case. Secondly, a constant average value of the dipole moment per unit step length was used, neglecting its dependence on island size and orientation. The value used was 9.5×10^6 D cm⁻¹ which corresponds to the dipole moment per unit step length of (100) steps of Au in a (111) Au surface.¹⁴ By inserting this value into the Helmholtz equation and using the data for the deviation of Φ deduced from the results of Fig. 3 we obtained an order of magnitude for the island perimeter, or, equivalently, of the density of islands of $10^{12} - 10^{13}$ per cm⁻².

D. XPS results for the Au/Pt(100)

The shifts observed in the binding energy of the 4*f* peaks of Au with increasing gold coverage (see Fig. 10) must reflect the changing average coordination number of the Au atoms. Several papers have already appeared in the literature where the photoelectron peaks due to surface and bulk atoms could be separated in energy.¹⁻⁵ The use of synchrotron radiation is the most suitable technique to observe these coordination effects due to the tunable energy and high resolution that can be achieved. Our low resolution (1.25 eV FWHM) is a serious drawback for these kinds of studies in semi-infinite crystals. However, in the case of atomic thickness overlayers, the photoelectron peaks of the adsorbate contain a very large proportion of low-coordination atoms, in such a way that its presence can be detected by measurable shifts of the compound unresolved photoelectron peak. The shifts shown

in Fig. 10 can then be explained in a simple way. Below $\Theta = 1$ we have essentially two types of Au atoms: Those with surface-type coordination, i.e., 4 for a (100) substrate, and the atoms located at the edges of the islands. Other types of low-coordination atoms also probably exist in small amounts, such as adatoms, vacancies, etc., but will not be considered in our crude model. In this model we assume that a certain number of islands per unit area expand two dimensionally as the gold coverage increases. The number of atoms located at the edges and at the center of these islands can then be easily calculated as a function of gold coverage Θ . For simplicity we have assumed square islands that increase until they coalesce. A compound XPS peak of gold was generated by superposition of three peaks centered at the binding energies corresponding to edge, surface, and bulk coordination (the last one only for $\Theta > 1$). Three parameters are thus left to fit the predicted relative shift to the experimental one. These parameters are number of nucleation centers or islands per cm², binding-energy difference for bulk and surface atoms, and binding-energy difference for edge and surface atoms. The best fit produced the continuous curve shown in Fig. 10 and corresponds to the following values of the parameters: island density $8 \pm 3 \times 10^{12}$ cm⁻², edge-to-surface 4*f* binding-energy shift 0.6 ± 0.2 eV, and surface-to-bulk binding-energy shift 0.4 ± 0.1 eV. The bulk component to the XPS peak of Au appears, as mentioned for $\Theta > 1$. Its contribution, however, has to be reduced on account of the attenuation of the photoelectrons by the Au overlayers. In the computation we used the experimental attenuation of the nearby Pt 4*f* peaks following the deposition of gold. As can be seen in the figure the fit is very good considering the crudeness of the model. It is worth noting that the figure obtained for the island density agrees with our previous estimate based on the work-function deviation from linearity.

Our data for the 4*f* core-level shift of Au in going from bulk-to-surface coordination agrees very well with the value of 0.40 ± 0.01 eV determined by Citrin *et al.*¹ and of 0.38 ± 0.01 eV determined by Heiman *et al.*⁴ The overall shift of $1.0 + 0.2$ eV from edge-to-bulk coordination is similar to the 0.75 eV determined by Van der Veen *et al.*⁵ for the step atoms relative to bulk atoms in Ir(332). These results show that it is possible to study the morphology of small clusters of metals by separating the contribution to the photoelectron spectra of the various types of atoms.

E. Ag deposited on Pt(100) and Pt(997)

As in the case of Au overlayers, Ag also displays changes in the intensity, energy position, and number of peaks in the photoemission curves. These changes reveal that here also the increasing size of the Ag islands first, and the formation of multilayers later, modifies the band structure due to the formation of new bonds. The region where the peaks are observed, from 4.5 to 6.5 eV corresponds to the energy position of the peaks originating from *d*-band transitions as observed by Roloff *et al.*¹⁹ Unlike the case of Au, however, no features above the *d*-band region were observed in that case. The work func-

tion of the clean metals decreased monotonically to reach final values of 4.71 ± 0.15 eV for the (100) substrate (at $\Theta \sim 3$) and 4.82 ± 0.15 eV for the (997) substrate (at $\Theta = 1.3$). Values reported in the literature are 4.64 ± 0.02 eV for Ag(100) (Ref. 20) and 4.74 eV for Ag(111).²⁰ The value for the (100) substrate of 4.71 eV is comparable with the reported one²¹ within the experimental error, whereas for the (997) substrate a somewhat high value was obtained,²² particularly as the more inhomogeneous Ag layer that is formed in that case⁹ seems to imply a still lower value of the work function. Since LEED studies were not carried out in that case, however, it is premature at this point to draw any definite conclusion.

The similarity with the case of Au is visible very clearly in the shift of the most tightly bound peak in the valence band (peak *d* in Fig. 9). This peak shows a shift of 0.6 eV in going from 0.1 to the monolayer, with most of the shift occurring in the monolayer range.

The small relative intensity of peak *d*, however, indicates that the center-of-gravity shift for the whole valence band of silver is much smaller than the observed 0.6 eV. In any case, the modification in the case of Ag appears to be restricted to the $0 < \Theta < 1$ region with no shift occurring above $\Theta = 1$. This result is consistent with the negligible surface-bulk core-level binding-energy shift of Ag that was measured by Citrin *et al.*¹

V. CONCLUSIONS

The photoelectron spectroscopy study of Au and Ag overlayers on Pt(100), Pt(111), and Pt(997) surfaces reveals

that both the valence-band and the core-level electron spectra are sensitive to the state of aggregation of the overlayer. The valence-band spectrum shows in all cases a narrowing for decreasing average coordination number. In the case of Au on Pt(100) this narrowing is reflected in the 0.6-eV shift of the Au $5d_{3/2}$ peak when Θ varies from 0 to 1. From $\Theta = 1$ to multilayer coverages an additional shift of 0.5 eV is observed for Au on the three substrate orientations. Other changes in the density of states occur when Θ grows above 1, reflecting the formation of inter-layer bonds.

The $4f$ core levels of Au deposited on Pt(100) show a shift of 0.6 eV towards higher binding energies when Θ varies from 0 to 1 and of 0.4 eV from 1 to 4. These shifts are the result of the changing contributions to the photoelectron peak of the Au atoms in various coordination environments. These are essentially bulk (for $\Theta > 1$) coordination, surface coordination, and island-edge coordination. The last two contributions are highly enhanced in the very thin overlayers studied here. The observed shifts and the deviation from linearity of the work-function data are all consistent with an island nucleation density of the order of $10^{12} - 10^{13}$ cm⁻² when $\Theta < 1$.

ACKNOWLEDGMENTS

This work was supported by the Director, Office of Basic Energy Science, Materials Science Division of the U.S. Department of Energy under Contract No. DE-AC03-76SF00098, and by the Spanish-American Cooperation Program.

*Permanent address: Instituto de Física del Estado Sólido del Consejo Superior de Investigaciones Científicas y Departamento de Física, Universidad Autónoma de Madrid, Cantoblanco, Madrid 34, Spain.

†Permanent address: University of Petroleum and Minerals, Dhahran, Saudi Arabia.

¹P. H. Citrin and G. K. Wertheim, Phys. Rev. Lett. **41**, 1425 (1978).

²T. M. Duc, C. Guillot, Y. Lassailly, J. Lecante, Y. Jugnet, and J. C. Vedrine, Phys. Rev. Lett. **43**, 789 (1979).

³J. F. van der Veen, F. J. Himpsel, and D. E. Eastman, Phys. Rev. Lett. **44**, 189 (1980).

⁴P. Heiman, J. F. van der Veen, and D. E. Eastman, Solid State Commun. **38**, 595 (1981).

⁵J. F. van der Veen, D. E. Eastman, A. M. Bradshaw, and S. Holloway, Solid State Commun. **39**, 1301 (1981).

⁶J. W. A. Sachtler, M. A. van Hove, J. P. Biberian, and G. A. Somorjai, Surf. Sci. **110**, 19 (1981).

⁷M. Pick, J. Davenport, M. Strongin, and J. Dienes, Phys. Rev. Lett. **41**, 286 (1979).

⁸D. Prigge, W. Schlenk, and E. Bauer, Surf. Sci. **123**, L698 (1982).

⁹P. W. Davies, M. A. Quinlan, and G. A. Somorjai, Surf. Sci. **121**, 290 (1982).

¹⁰J. W. A. Sachtler, M. A. van Hove, J. P. Biberian, and G. A.

Somorjai, Phys. Rev. Lett. **45**, 1601 (1980).

¹¹M. Salmerón, S. Ferrer, M. Jassar, and G. A. Somorjai, Phys. Rev. B **28**, 1158 (1983).

¹²P. Heimann, J. Hermanson, H. Miosga, and H. Neddermeyer, Phys. Rev. Lett. **43**, 1757 (1979).

¹³H. P. Bonzel, C. R. Helms, and S. Kelemen, Phys. Rev. Lett. **35**, 1237 (1975).

¹⁴K. Besocke, B. Krahl-Urban, and H. Wagner, Surf. Sci. **68**, 39 (1977).

¹⁵T. M. Gardiner, H. M. Kramer, and E. Bauer, Surf. Sci. **112**, 181 (1981).

¹⁶B. E. Nieuwenhuys and W. M. H. Sachtler, Surf. Sci. **34**, 317 (1973).

¹⁷H. C. Potter and J. M. Blakely, J. Vac. Sci. Technol. **12**, 635 (1975).

¹⁸J. Hulse, J. Küppers, K. Wandelt, and G. Ertl, Appl. Surf. Sci. **6**, 453 (1980).

¹⁹H. F. Roloff and H. Neddermeyer, Solid State Commun. **21**, 561 (1977).

²⁰A. W. Dweydari and C. H. B. Mee, Phys. Status Solidi A **27**, 223 (1975); **17**, 247 (1973).

²¹P. H. Citrin and G. K. Wertheim, Phys. Rev. B **27**, 3176 (1983).

²²M. G. Mason, Phys. Rev. B **27**, 748 (1983).